Baryon and lepton number violation from gravitational waves

Bartosz Fornal and Barmak Shams Es Haghi

Department of Physics and Astronomy, University of Utah, Salt Lake City, Utah 84112, USA

We describe a unique gravitational wave signature for a class of models with a vast hierarchy between the symmetry breaking scales. The unusual shape of the signal is a result of the overlapping contributions to the stochastic gravitational wave background from cosmic strings produced at a high scale and a cosmological phase transition at a low scale. We apply this idea to a simple model with gauged baryon and lepton numbers, in which the high-scale breaking of the lepton number is motivated by the seesaw mechanism for the neutrinos, whereas the low scale of baryon number breaking is required by the observed dark matter relic density. The novel signature can be searched for in upcoming gravitational wave experiments.

I. INTRODUCTION

Gravitational wave detectors opened the door to an entirely new set of opportunities for probing unexplored avenues in physics and astronomy. Many astrophysical discoveries have already been made using solely the data gathered by LIGO [1] and Virgo [2] in their initial runs. One can only imagine what will be learned from future detectors such as LISA [3], DECIGO [4], Cosmic Explorer (CE) [5], Einstein Telescope (ET) [5], and Big Bang Observer (BBO) [6]. Interestingly, gravitational wave experiments may not only reveal information about black hole and neutron star mergers, but they can also provide a deep insight into the particle physics of the early universe.

The shape of the stochastic gravitational wave background is the key to unraveling the symmetry breaking pattern in the first instances after the big bang. It enables us to explore the physics at the very high energy scale, inaccessible directly in any other experiment and, so far, probed only indirectly, e.g., via proton decay searches. Thus, a discovery of a gravitational wave signal from the early universe would provide invaluable insight into the UV completion of the Standard Model. The two main sources of such gravitational waves are cosmological phase transitions and cosmic strings.

Depending on the parameters of the scalar potential, upon symmetry breaking at early times the universe might have been trapped in a vacuum that became metastable as the temperature dropped. In the presence of a potential barrier separating this false vacuum from the true vacuum, a first order phase transition would occur, nucleating bubbles of true vacuum which expanded and populated the universe. This, in turn, would lead to a production of gravitational waves with a characteristic bumplike shape in the spectrum. Indeed, such signals have been analyzed in the context of various particle physics models (see, e.g., [7–31]).

On the other hand, symmetry breaking can also lead to the production topological defects such as cosmic strings, as it happens, e.g., in models with a complex scalar field charged under a U(1) gauge group. A network of cosmic strings is a long-lasting source of gravitational waves and gives rise to a spectrum which, to a good approximation, is flat in a wide range of frequencies. Such cosmic string signatures have also been considered in many models (see, e.g., [32–42]).

For a single broken U(1) gauge group, the cosmic string contribution is negligible in the frequency range relevant for the gravitational wave signal of a phase transition. However, if cosmic strings were produced by a high-scale breaking of $U(1)_{high}$, whereas the first order phase transition was triggered by the breaking of a different $U(1)_{low}$ at a much lower energy scale, the two contributions could end up comparable at frequencies corresponding to the $U(1)_{low}$ breaking.

In this paper, we propose to look precisely for such a combined signature of a phase transition and cosmic strings. This is naturally realized in models with a seesaw mechanism, in which the large mass of the right-handed neutrinos arises from lepton number breaking at a scale $v_L \sim 10^{10}$–10^{15} GeV. In a certain frequency band, the resulting cosmic string signal can have a similar magnitude to that of a phase transition happening at a scale $v_B \sim 10^3$–10^5 GeV. For a particular realization of this scenario, we focus on a simple model with gauged baryon and lepton numbers [43], where the high-scale lepton number breaking is motivated by the seesaw mechanism,

whereas the low scale of baryon number breaking is required to explain the dark matter relic abundance.

There are several reasons for gauging baryon and lepton numbers and breaking them spontaneously. In the Standard Model, B and L are accidental global symmetries. Such symmetries, however, cannot be fundamental in a consistent theory of quantum gravity, unlike gauge symmetries [44]. Another motivation comes from the matter-antimatter asymmetry of the universe, which requires the baryon number to be broken beyond the nonperturbative effects mediated by the electroweak sphalerons. Early attempts of gauging $U(1)_B$ and $U(1)_L$ were made in [45–49], but phenomenologically viable models consistent with LHC constraints were constructed only recently [43,50–54] and can naturally account for the nonobservation of proton decay, small neutrino masses, dark matter, and the matter-antimatter asymmetry. This idea was further generalized to the non-Abelian case and partially unified theories in [55–58].

Although the focus of this paper is on the model constructed in [43], our proposed signature is much more general and can be realized in other models with two U(1) gauge groups broken at vastly different scales, not necessarily associated with baryon or lepton number.

II. GAUGING BARYON AND LEPTON NUMBER

The model we consider is based on the gauge group

$$SU(3)_c \times SU(2)_L \times U(1)_Y \times U(1)_B \times U(1)_L. \quad (1)$$

The charges under $U(1)_B$ and $U(1)_L$ of the Standard Model particles are the same as their standard B and L assignments. The requirement of gauge anomaly cancellation implies the existence of new fermion fields. There are many possible choices for these extra fields, with various hypercharge and $U(1)_B$ and $U(1)_L$ charge assignments. Since the particular choice of the new fermions or their charges does not qualitatively impact our results, we consider the original set of fields proposed in [43].

The Standard Model is extended with three families of right-handed neutrinos ν_{iR} and the following single set of leptobaryonic fermions:

$$\Psi_L = \left(1, 2, \frac{1}{2}, B_1, L_1\right), \qquad \Psi_R = \left(1, 2, \frac{1}{2}, B_2, L_2\right),$$

$$\eta_R = (1, 1, 1, B_1, L_1), \qquad \eta_L = (1, 1, 1, B_2, L_2),$$

$$\chi_R = (1, 1, 0, B_1, L_1), \qquad \chi_L = (1, 1, 0, B_2, L_2), \quad (2)$$

with the relations $B_2 - B_1 = 3$ and $L_2 - L_1 = 3$ satisfied. We are going to assume $B_1 = L_1 = -1$ and $B_2 = L_2 = 2$.

Two new scalar fields are also introduced into the model,

$$\Phi_L = (1, 1, 0, 0, -2), \qquad \Phi_B = (1, 1, 0, -3, -3). \quad (3)$$

The gauge group $U(1)_L$ is broken by the vacuum expectation value (VEV) of the field Φ_L at a high scale, whereas $U(1)_B$ is broken by the VEV of Φ_B at a lower scale,

$$\langle \Phi_L \rangle = \frac{v_L}{\sqrt{2}}, \qquad \langle \Phi_B \rangle = \frac{v_B}{\sqrt{2}}, \quad (4)$$

with a large hierarchy between them, and with respect to the Standard Model Higgs H VEV $v \approx 246$ GeV,

$$v_L \gg v_B \gg v. \quad (5)$$

The Lagrangian terms describing the interactions of the new fermions with scalars are

$$\mathcal{L} \supset Y_\Psi \bar{\Psi}_L \Psi_R \Phi_B + Y_\eta \bar{\eta}_R \eta_L \Phi_B + Y_\chi \bar{\chi}_R \chi_L \Phi_B$$
$$+ y_{\eta_R} \bar{\Psi}_L H \eta_R + y_{\eta_L} \bar{\Psi}_R H \eta_L + y_{\chi_R} \bar{\Psi}_L H \chi_R$$
$$+ y_{\chi_L} \bar{\Psi}_R H \chi_L + y_\nu \bar{l}_L \tilde{H} \nu_R + Y_\nu \nu_R \nu_R \Phi_L + \text{H.c.} \quad (6)$$

The only fermions that couple to Φ_L are the right-handed neutrinos. Because of the large hierarchy between the symmetry breaking scales, one can ignore the effect of terms involving H on the fermion masses.

The scalar potential for Φ_L and Φ_B is given by

$$V(\Phi_L, \Phi_B) = -\mu_L^2 |\Phi_L|^2 + \lambda_L |\Phi_L|^4 - \mu_B^2 |\Phi_B|^2 + \lambda_B |\Phi_B|^4, \quad (7)$$

where we have left out the possible cross terms between the fields Φ_L, Φ_B, and H, assuming that the corresponding coefficients are small.

The Standard Model covariant derivative is extended to

$$D_\mu = D_\mu^{SM} + ig_B B_\mu B + ig_L L_\mu L. \quad (8)$$

After symmetry breaking, the fields B_μ and L_μ give rise to the gauge bosons Z_B and Z_L that couple exclusively to baryons and leptons, respectively. Their masses are

$$m_{Z_B} = 3g_B v_B, \qquad m_{Z_L} = 2g_L v_L. \quad (9)$$

Since $U(1)_B$ and $U(1)_L$ are not unified with the Standard Model gauge group, the gauge couplings g_B and g_L are free parameters, similar to λ_B, λ_L, and the new Yukawas.

The breaking of $U(1)_L$ results in a $\Delta L = 2$ mass term for the right-handed neutrinos, which leads to the type I seesaw mechanism. Assuming the Yukawa couplings $y_\nu \sim \mathcal{O}(10^{-2})$ and $Y_\nu \sim \mathcal{O}(1)$, the measured neutrino mass splittings are naturally explained if the scale of lepton number breaking is

$$v_L \approx 10^{11} \text{ GeV}. \quad (10)$$

The breaking of $U(1)_B$ leads to baryon number violation, but only by three units, $\Delta B = 3$. This implies that proton is absolutely stable in this model. In addition, since the

lowest-dimensional baryon number violating operator appears at dimension 19,

$$\mathcal{O} \sim \frac{(u_R u_R d_R e_R)^3 \Phi_B}{\Lambda^{15}}, \tag{11}$$

the resulting $\Delta B = 3$ processes are highly suppressed.

Interestingly, after $U(1)_B$ and $U(1)_L$ breaking, an accidental global symmetry remains in the new sector, under which the leptobaryons transform as

$$\Psi_{L,R} \to e^{i\alpha}\Psi_{L,R}, \qquad \eta_{L,R} \to e^{i\alpha}\eta_{L,R},$$
$$\chi_{L,R} \to e^{i\alpha}\chi_{L,R}. \tag{12}$$

This implies the stability of the lightest leptobaryon. Assuming $Y_\chi < Y_{\Psi,\eta}$, the lightest new field is χ. As a Standard Model singlet, χ becomes a viable dark matter candidate.

If χ is indeed a dark matter particle, the cross section for its annihilation needs to be consistent with the observed dark matter relic density $h^2\Omega_{\mathrm{DM}} = 0.12$ [59]. Since the annihilation proceeds via the s-channel $\chi\bar{\chi} \to Z_B^* \to q\bar{q}$, and the mass of the gauge boson Z_B depends on the symmetry breaking scale, this introduces a nontrivial relation between the parameters v_B, g_B, and Y_χ. As pointed out in [53] (see also [60]), with $B_1 + B_2 = 1$ this imposes the upper bound

$$g_B v_B \lesssim 20 \text{ TeV}. \tag{13}$$

In the analysis of the phase transition resulting from $U(1)_B$ breaking in Sec. IV we adopt $\lambda_B \sim 10^{-2}$. The gravitational wave signal is then maximized for $g_B \sim 0.3$. Therefore, as a benchmark scenario we assume the parameter values,

$$v_B = 20 \text{ TeV}, \quad g_B = 0.3, \quad \lambda_B = 10^{-2}, \quad Y_\chi = 0.6, \tag{14}$$

with $Y_{\Psi,\eta}$ slightly larger than Y_χ, so that χ remains the lightest leptobaryon. In this benchmark model $M_{Z_B} \sim 20$ TeV, well beyond the LHC reach. However, a phase transition signal associated with symmetry breaking at this scale is within the reach of upcoming gravitational wave experiments.

III. COSMIC STRINGS FROM $U(1)_L$ BREAKING

The spontaneously broken gauge symmetry $U(1)_L$ can lead to gravitational wave production in two very different ways: (1) within a very short timescale during a phase transition via sound waves, bubble collisions, and turbulence (as discussed in Sec. IV), or (2) in a long-term process resulting from the dynamics of the produced cosmic strings. Since the frequencies of the type (1) signal for a high scale v_L are inaccessible via gravitational detectors in

the foreseeable future, we consider only the cosmic string signature of $U(1)_L$ breaking, since it extends to lower frequencies.

A. Cosmic string network

Cosmic strings may be generated during the breaking of $U(1)_L$ through the Kibble mechanism [61]. They are topological defects corresponding to one-dimensional field configurations where the symmetry remains unbroken. The produced cosmic string network is characterized by the string tension μ (energy per unit length). It is related to the symmetry breaking scale v_L via [38,62]

$$G\mu = 2\pi\left(\frac{v_L}{M_P}\right)^2, \tag{15}$$

where G is the gravitational constant, $M_P = 1.22 \times 10^{19}$ GeV is the Planck mass, and we assumed that the winding number $n = 1$. Measurements of the cosmic microwave background constrain the string tension to be $G\mu \lesssim 10^{-7}$ [63].

The cosmic string network experiences two competing contributions to its dynamics: stretching (due to the expansion of the universe) and formation of string loops (when long strings intersect and intercommute). The string loops themselves are unstable: they oscillate and eventually decay. The combination of the two effects results in a *scaling regime* that consists of a small number of Hubble-length strings and a large number of string loops [64–68]. The energy is continuously transferred from long strings to loops, and eventually to radiation or particles, constituting a fixed fraction of the total energy density of the universe [69].

The dominant decay channel of string loops is gravitational radiation [70,71]. In particular, powerful bursts of gravitational waves are expected to be produced by cusps and kinks propagating along the string loops, as well as kink-kink collisions. The superposition of these bursts results in a stochastic gravitational wave background. To calculate the corresponding signal, we follow the framework adopted in [35,38].

B. String dynamics

Let us consider a cosmic string loop created at time t_i and of length $l(t_i) = \alpha t_i$, where α is an approximately constant loop size parameter. We assume $\alpha = 0.1$, as this provides a good approximation for the loop size distribution determined in [32,72]. While the loop oscillates, it emits gravitational waves with frequencies

$$\tilde{\nu} = \frac{2k}{l}, \quad \text{where } k \in \mathbb{Z}^+. \tag{16}$$

In the current epoch, this corresponds to $\nu = a(\tilde{t})/a(t_0)\tilde{\nu}$, where a is the scale factor of the universe, $\tilde{t}$ is the emission time, and t_0 denotes the time today.

The spectrum of gravitational waves emitted from a single loop is given by [32,72]

$$P_{\text{CS}}^{(k,n)} = \frac{\Gamma G \mu^2 k^{-n}}{\sum_{p=1}^{\infty} p^{-n}}, \qquad (17)$$

where $n = \frac{4}{3}, \frac{5}{3}, 2$ corresponds to the contribution from cusps, kinks, and kink-kink collisions, respectively, and $\Gamma \simeq 50$ [73]. Because of the emission of gravitational waves, the loop shrinks,

$$l(\tilde{t}) = \alpha t_i - \Gamma G \mu (\tilde{t} - t_i), \qquad (18)$$

and decays after the time $\tau = \alpha t_i / (\Gamma G \mu)$. Furthermore, it was shown in [72] that only $\mathcal{F}_\alpha \approx 10\%$ of the loops contribute to the gravitational wave signal.

The model dependence enters through the assumption regarding the loop distribution function $f(l, t) dl$, which describes the number density of loops with an invariant length in the range $(l, l + dl)$ at the cosmic time t. We adopt the framework of the velocity-dependent one-scale model [74–76], which describes the evolution of a string network in terms of only two parameters: the mean string velocity and the correlation length. In the scaling solution regime, for which those parameters become constant, one arrives at

$$f(l, t_i) = \frac{\sqrt{2} C_{\text{eff}}}{\alpha t_i^4} \delta(l - \alpha t_i), \qquad (19)$$

where $C_{\text{eff}} = 5.4$ for the radiation era and $C_{\text{eff}} = 0.39$ for matter domination [35].

C. Gravitational wave signal

The dynamics of the cosmic string network generates the stochastic gravitational wave background given by [35,38]

$$h^2 \Omega_{\text{CS}}(\nu) = \frac{2h^2 \mathcal{F}_\alpha}{\rho_c \nu \alpha^2} \sum_{k,n} k P_{\text{CS}}^{(k,n)} \int_{t_F}^{t_0} d\tilde{t} \, \frac{C_{\text{eff}}(t_{i,k})}{t_{i,k}^4}$$
$$\times \left(\frac{a(\tilde{t})}{a(t_0)} \right)^5 \left(\frac{a(t_{i,k})}{a(\tilde{t})} \right)^3 \Theta(t_{i,k} - t_F). \qquad (20)$$

In the expression above ρ_c is the critical density, Θ is the Heaviside function, t_F is the time of the cosmic string network formation (i.e., when the energy scale of the universe is equal to the string tension, $\sqrt{\rho(t_F)} = \mu$ [38]), $t_{i,k}$ is the time of the loop production,

$$t_{i,k} \equiv t_{i,k}(\tilde{t}, \nu) = \frac{1}{\alpha} \left(\frac{2k}{\nu} \frac{a(\tilde{t})}{a(t_0)} + \Gamma G \mu \tilde{t} \right), \qquad (21)$$

$\tilde{t}$ is the time of the gravitational wave emission, and t_0 is the time today. We have also assumed $G\mu \ll \alpha$. Following
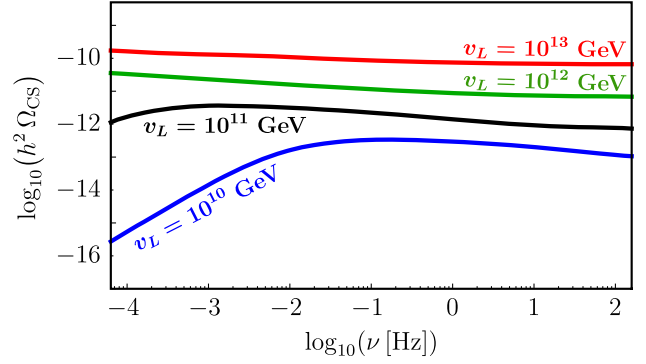

FIG. 1. Stochastic gravitational wave background from the cosmic string network produced from gauged $U(1)_L$ breaking for several choices of the scale v_L.

[35,38], we consider only the contribution of the cusps to the gravitational wave signal.

Figure 1 shows the resulting cosmic string contribution $h^2 \Omega_{\text{CS}}$ to the stochastic gravitational wave background, calculated using Eq. (20), for several choices of the $U(1)_L$ breaking scale, and in the frequency range relevant for upcoming gravitational wave experiments.

IV. PHASE TRANSITION FROM $U(1)_B$ BREAKING

In this section we derive the spectrum of the stochastic gravitational wave background generated by sound waves and magnetohydrodynamic turbulence from the first order phase transition triggered by gauged baryon number breaking. For the sound wave contribution we adopt a novel estimate of the suppression factor recently derived in [77], which considerably weakens the gravitational wave signal.

A. Effective potential

The large hierarchy between the scales, as given by Eq. (5), implies that the effective potential for the background field $\phi_B \equiv \sqrt{2} \text{Re}(\Phi_B)$ can be considered independently from the other background fields. The three types of contributions to the potential are tree-level, one-loop, and finite temperature.

The tree-level part is

$$V_{\text{tree}}(\phi_B) = -\frac{1}{2} \lambda_B v_B^2 \phi_B^2 + \frac{1}{4} \lambda_B \phi_B^4, \qquad (22)$$

where we used the relation between the parameters satisfied at the minimum, $\mu_B = v_B \sqrt{\lambda_B}$.

The one-loop Coleman-Weinberg contribution, adopting the cutoff regularization scheme and matching the one-loop and tree-level minima, can be written as

$$V_{1-\text{loop}}(\phi_B) = \sum_i \frac{n_i}{32\pi^2} \left\{ m_i^4(\phi_B) \left[\log\left(\frac{m_i(\phi_B)}{m_i(v_B)}\right) - \frac{3}{4} \right] \right.$$
$$\left. + m_i^2(\phi_B) m_i^2(v_B) \right\}, \tag{23}$$

where the sum is over all particles coupling to ϕ_B, while n_i is the number of degrees of freedom of a given particle, with a minus sign for fermions. For the Goldstone boson χ_B, one needs to replace $m_{\chi_B}(v_B) \to m_{\phi_B}(v_B)$. The background field-dependent masses are

$$m_{Z_B}(\phi_B) = 3g_B\phi_B, \qquad m_{\phi_B}(\phi_B) = [\lambda_B(3\phi_B^2 - v_B^2)]^{1/2},$$
$$m_{\chi_B}(\phi_B) = [\lambda_B(\phi_B^2 - v_B^2)]^{1/2}, \qquad m_\Psi(\phi_B) = Y_\Psi\phi_B/\sqrt{2},$$
$$m_\eta(\phi_B) = Y_\eta\phi_B/\sqrt{2}, \qquad m_\chi(\phi_B) = Y_\chi\phi_B/\sqrt{2}. \tag{24}$$

The finite temperature part of the effective potential is

$$V_{\text{temp}}(\phi_B, T)$$
$$= \frac{T^4}{2\pi^2} \sum_i n_i \int_0^\infty dy\, y^2 \log\left(1 \mp e^{-\sqrt{m_i^2(\phi_B)/T^2 + y^2}} \right)$$
$$+ \frac{T}{12\pi} \sum_j n_j' \{ m_j^3(\phi_B) - [m_j^2(\phi_B) + \Pi_j(T)]^{\frac{3}{2}} \}. \tag{25}$$

In the expression above, the sum over i includes all particles coupling to ϕ_B, whereas that over j includes only bosons. The plus/minus sign corresponds to fermions/ bosons. Ignoring the terms suppressed by small λ_B, the thermal masses are

$$\Pi_{\phi_B}(T) = \Pi_{\chi_B}(T) = \frac{9}{4} g_B^2 T^2, \qquad \Pi_{Z_B}^L(T) = \frac{14}{3} g_B^2 T^2, \tag{26}$$

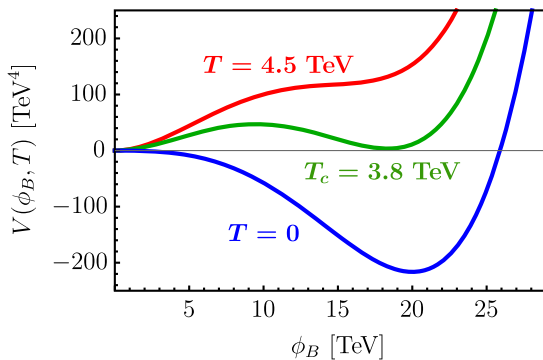where the superscript L denotes longitudinal components.

FIG. 2. Plot of the effective potential $V_{\text{eff}}(\phi_B, T) - V_{\text{eff}}(0, T)$ for the choice of parameters in Eq. (14) and several temperatures.

The full effective potential is given by

$$V_{\text{eff}}(\phi_B, T) = V_{\text{tree}}(\phi_B) + V_{1-\text{loop}}(\phi_B) + V_{\text{temp}}(\phi_B, T). \tag{27}$$

It is shown in Fig. 2 for the benchmark scenario in Eq. (14). A strong first order phase transition occurs, since there is a barrier separating the false vacuum from the true one.

B. Phase transition

When a patch of the universe tunnels from the false vacuum to the true vacuum, a bubble is formed and starts expanding. The nucleation rate of such bubbles per unit volume is [78]

$$\Gamma(T) \sim T^4 \exp\left(-\frac{S(T)}{T}\right), \tag{28}$$

where the Euclidean action $S(T)$ is given by

$$S(T) = 4\pi \int dr\, r^2 \left[\frac{1}{2} \phi_b'(r)^2 + V_{\text{eff}}(\phi_b, T) \right] \tag{29}$$

and $\phi(r)$ is the solution of the expanding bubble equation with appropriate boundary conditions,

$$\phi_b''(r) + \frac{2}{r} \phi_b'(r) - \left.\frac{dV_{\text{eff}}(\phi, T)}{d\phi}\right|_{\phi=\phi_b} = 0,$$
$$\phi_b'(0) = 0, \qquad \phi_b(\infty) = \phi_{\text{true}}. \tag{30}$$

The onset of the phase transition occurs at the nucleation temperature T_* at which $\Gamma(T_*) \approx H^4$. Using Eq. (28), this condition can be rewritten as

$$4\log\left(\frac{M_P}{T_*}\right) \approx \frac{S(T_*)}{T_*}. \tag{31}$$

A phase transition is fully described by four parameters: the bubble wall velocity v_w, the nucleation temperature T_*, the inverse of its duration $\tilde{\beta}$,

$$\tilde{\beta} = T_* \left.\frac{d}{dT}\left(\frac{S(T)}{T}\right)\right|_{T=T_*}, \tag{32}$$

and the strength of the transition α,

$$\alpha = \frac{\rho_{\text{vac}}(T_*)}{\rho_{\text{rad}}(T_*)}. \tag{33}$$

In the expression above

$$\rho_{\mathrm{vac}}(T_*) = V_{\mathrm{eff}}(\phi_{\mathrm{false}}, T_*) - V_{\mathrm{eff}}(\phi_{\mathrm{true}}, T_*)$$
$$- T_* \left. \frac{\partial[V_{\mathrm{eff}}(\phi_{\mathrm{false}}, T) - V_{\mathrm{eff}}(\phi_{\mathrm{true}}, T)]}{\partial T} \right|_{T=T_*}$$

$$(34)$$

is the energy density of the false vacuum and

$$\rho_{\mathrm{rad}}(T_*) = \frac{\pi^2}{30} g_*(T_*) T_*^4 \qquad (35)$$

is the radiation energy density, with $g_*(T_*)$ being the number of relativistic degrees of freedom at the time of the transition.

Out of the four parameters v_w, T_*, $\tilde{\beta}$, α, only the bubble wall velocity does not depend on the shape of the effective potential, and we will set it to $v_w \approx 0.7c$ (for a detailed discussion of the possible choices see [79]). For the benchmark scenario in Eq. (14) the nucleation temperature is $T_* \approx 600$ GeV and $g_*(T_*) \approx 107$, since all degrees of freedom beyond the Standard Model are nonrelativistic at this T_*.

C. Gravitational wave signal

The sound wave contribution to the gravitational wave spectrum is given by [80,81]

$$h^2 \Omega_s(\nu) \approx (1.86 \times 10^{-5}) \frac{\left(\frac{\nu}{\nu_s}\right)^3}{[1 + 0.75(\frac{\nu}{\nu_s})^2]^{\frac{7}{2}}}$$
$$\times \frac{v_w}{\tilde{\beta}} \left(\frac{\kappa_s \alpha}{\alpha + 1}\right)^2 \left(\frac{100}{g_*}\right)^{\frac{1}{3}} \Upsilon, \qquad (36)$$

where the parameter κ_s (the fraction of the latent heat transformed into the bulk motion of the plasma [79]) and the peak frequency ν_s are

$$\kappa_s \approx \frac{\alpha}{0.73 + 0.083\sqrt{\alpha} + \alpha},$$

$$\nu_s \approx (1.9 \times 10^{-4} \text{ Hz}) \left(\frac{g_*}{100}\right)^{\frac{1}{6}} \frac{\tilde{\beta}}{v_w} \left(\frac{T_*}{1 \text{ TeV}}\right), \quad (37)$$

and Υ is the suppression factor adopted from [77],

$$\Upsilon = 1 - \left[1 + \frac{8\pi^{\frac{1}{3}}}{\sqrt{3}} \frac{v_w}{\tilde{\beta}} \left(\frac{\alpha \kappa_s}{\alpha + 1}\right)^{-\frac{1}{2}}\right]^{-\frac{1}{2}}. \qquad (38)$$

This leads to a stronger suppression of the sound wave signal than previously estimated [82–84], weakening it by nearly 2 orders of magnitude.

The contribution to the gravitational wave spectrum arising from bubble collisions, $h^2 \Omega_c(\nu)$, was studied in [81,85,86]. Adopting the corresponding formula for $h^2 \Omega_c$, the effect of bubble wall collisions can be comparable to the

sound wave contribution or even dominate it in certain frequency ranges. However, as discussed in [84], it has recently been argued that the gravitational radiation from the collision phase might actually be swamped by the radiation generated by the motion of the fluid in later phases of the transition. Therefore, in what follows, we neglect the effect of bubble wall collisions. We note that this does not qualitatively affect our results.

The remaining contribution from turbulence is [87]

$$h^2 \Omega_t(\nu) \approx (3.35 \times 10^{-4}) \frac{\left(\frac{\nu}{\nu_t}\right)^3}{(1 + \frac{8\pi\nu}{h_*})(1 + \frac{\nu}{\nu_t})^{\frac{11}{3}}}$$
$$\times \frac{v_w}{\tilde{\beta}} \left(\frac{\epsilon \kappa_s \alpha}{\alpha + 1}\right)^{\frac{3}{2}} \left(\frac{100}{g_*}\right)^{\frac{1}{3}}, \qquad (39)$$

where we adopt $\epsilon = 0.05$ [81] and

$$h_* = (1.7 \times 10^{-4} \text{ Hz}) \left(\frac{g_*}{100}\right)^{\frac{1}{6}} \left(\frac{T_*}{1 \text{ TeV}}\right),$$

$$\nu_t = 1.64 \frac{\tilde{\beta}}{v_w} h_*. \qquad (40)$$

Figure 3 shows the contributions to the stochastic gravitational wave background from $U(1)_B$ breaking that originate from sound waves and magnetohydrodynamic turbulence, for the benchmark scenario in Eq. (14) and in the frequency range relevant for upcoming gravitational wave experiments.

To determine how likely it is for the phase transition from $U(1)_B$ breaking to produce an observable gravitational wave signal, we performed a scan over the relevant parameters. Figure 4 shows the region of parameter space for the gauge coupling g_B versus the quartic coupling λ_B that yields a first order phase transition (for $v_B = 20$ TeV), giving rise to a signal detectable at LISA, DECIGO, and the Big Bang Observer, with a signal-to-noise ratio greater than
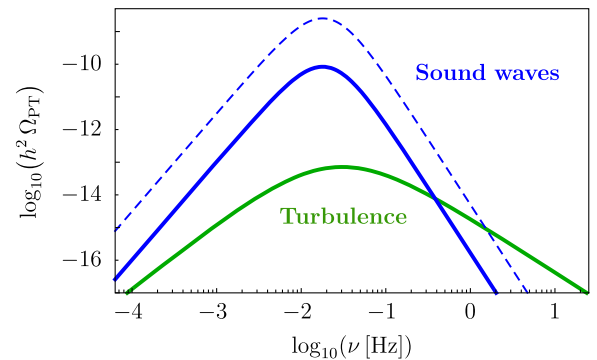

FIG. 3. Stochastic gravitational wave background produced by sound waves and turbulence during a first order phase transition triggered by the breaking of gauged $U(1)_B$, for the benchmark scenario in Eq. (14). The dashed line corresponds to the signal from sound waves without the suppression factor Υ.
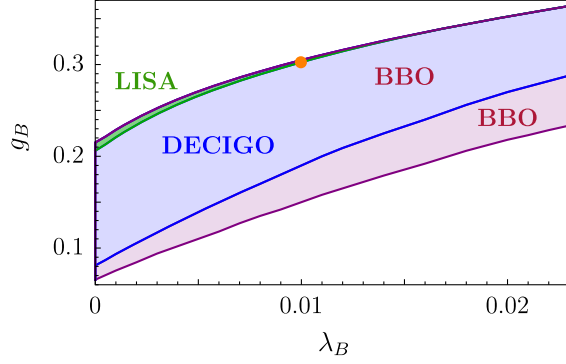
FIG. 4. The parameter space region (λ_B, g_B) for which a phase transition triggered by $U(1)_B$ breaking with $v_B = 20$ TeV gives rise to a gravitational wave signal detectable at LISA (green), DECIGO (green and blue), and BBO (green, blue, and purple) with a signal-to-noise ratio greater than five after one year of collecting data. The orange dot denotes the benchmark parameters used in Fig. 5.

five after one year of collecting data. A sizable portion of parameter space leads to a measurable signal.

V. GRAVITATIONAL WAVE SIGNATURE

Figure 5 shows the combined gravitational wave signature of the cosmic string network produced at the high scale and a first order phase transition that occurred at the low scale. The plot was made for the model with gauged baryon and lepton numbers with $v_L = 10^{11}$ GeV and the parameter values as in Eq. (14). The expected signal is flat throughout a wide range of frequencies and contains a characteristic bumplike feature, which distinguishes it from pure seesaw signatures.

The position of the bump depends linearly on the nucleation temperature; for a higher $U(1)_B$ breaking scale the phase transition appears at higher frequencies. The parameter $\tilde{\beta}$ affects both the position of the peak and its height, whereas the parameter α governs only its height; a larger $\tilde{\beta}$ corresponds to higher frequencies and a weaker signal, whereas a larger α implies a stronger signal.

The breadth of the signature across many frequencies places it within the reach of nearly all upcoming gravitational wave detectors. The high-frequency flat part of the signal can be searched for in experiments like the Cosmic Explorer and the Einstein Telescope, whereas the low-frequency part including the bump feature is within the reach of LISA, the Big Bang Observer, and DECIGO. The signal is clearly distinguishable from a pure cosmic string signature (shown as the brown dotted line) and from a pure phase transition signature (denoted by the brown dashed line).

VI. SUMMARY

We have recently entered an extremely exciting time when progress in particle physics may actually come from classical gravity measurements. Gravitational wave detectors offer a very promising probe of the early universe and may provide information on the structure of the theory at high scales, well above the LHC reach and inaccessible directly in any other existing experiment. There are generally two kinds of particle physics signatures that can be searched for via gravitational wave measurements, and that fall within the sensitivity of near-future gravitational wave experiments.

Signals of the first type arise from cosmic phase transitions, and are produced abruptly by sound waves,
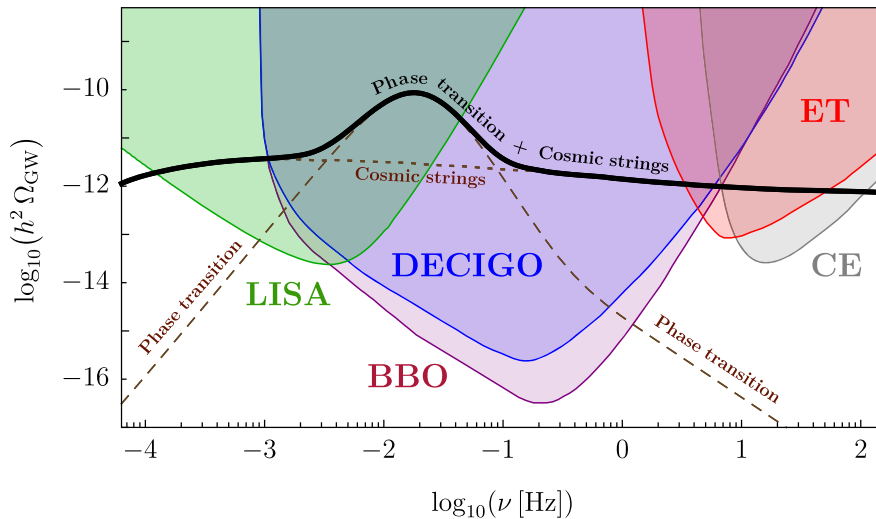

FIG. 5. Stochastic gravitational wave signature of the model with gauged baryon and lepton numbers for $v_B = 20$ TeV and $v_L = 10^{11}$ GeV (black solid line). Sensitivities of future detectors are also shown: Big Bang Observer [88] (purple), DECIGO [88] (blue), LISA (in the C1 configuration) [81] (green), Cosmic Explorer [5] (gray), and Einstein Telescope [89] (red). The dashed line denotes the contribution from the phase transition associated with $U(1)_B$ breaking, whereas the dotted line corresponds to the cosmic string signal from $U(1)_L$ breaking.

bubble collisions, and magnetohydrodynamic turbulence. They exhibit a bumplike shape, with the peak frequency determined by the symmetry breaking scale. The second class of signals comes from the dynamics of the cosmic string network, produced during a phase transition, but sourcing gravitational radiation throughout a long period after its formation. Those signals are flat and stretch out across a wide range of frequencies.

In this paper, we considered the possibility of the two types of signals coexisting and giving rise to a new type of signature—a flat spectrum with a bump feature—which is within the reach of upcoming gravitational wave experiments. We pointed out that such signatures occur generically in models with two or more gauge symmetries that are broken at vastly separated scales. We analyzed this scenario in the context of a model with gauged baryon and lepton numbers, where the high-scale breaking of the lepton number is motivated by the seesaw mechanism for the neutrinos, whereas the breaking of the baryon number is confined to a much lower scale by the observed dark matter relic abundance. The flat part of the resulting spectrum is within the reach of the Cosmic Explorer and Einstein Telescope, whereas the bump feature falls within the sensitivity of LISA, the Big Bang Observer, and DECIGO.

Such a cosmic search for a combined signature of baryon and lepton number violation is complementary to collider efforts. An observation of the gravitational wave signal proposed here would be a strong motivation for building the 100 TeV collider, which could independently search for the leptophobic gauge boson associated with baryon number breaking. Such a discovery would also imply the necessity of revisiting the ideas about grand unification, once again showing that nature is full of surprises.

ACKNOWLEDGMENTS

[1] J. Aasi *et al.* (LIGO Scientific Collaboration), Advanced LIGO, Classical Quantum Gravity **32**, 074001 (2015).

[2] F. Acernese *et al.* (Virgo Collaboration), Advanced Virgo: A second-generation interferometric gravitational wave detector, Classical Quantum Gravity **32**, 024001 (2015).

[3] P. Amaro-Seoane *et al.* (LISA Collaboration), Laser interferometer space antenna, arXiv:1702.00786.

[4] S. Kawamura *et al.*, The Japanese space gravitational wave antenna: DECIGO, Classical Quantum Gravity **28**, 094011 (2011).

[5] D. Reitze *et al.*, Cosmic Explorer: The U.S. contribution to gravitational-wave astronomy beyond LIGO, Bull. Am. Astron. Soc. **51**, 035 (2019).

[6] J. Crowder and N. J. Cornish, Beyond LISA: Exploring future gravitational wave missions, Phys. Rev. D **72**, 083005 (2005).

[7] R. Apreda, M. Maggiore, A. Nicolis, and A. Riotto, Gravitational waves from electroweak phase transitions, Nucl. Phys. **B631**, 342 (2002).

[8] C. Grojean and G. Servant, Gravitational waves from phase transitions at the electroweak scale and beyond, Phys. Rev. D **75**, 043507 (2007).

[9] L. Leitao, A. Megevand, and A. D. Sanchez, Gravitational waves from the electroweak phase transition, J. Cosmol. Astropart. Phys. 10 (2012) 024.

[10] P. Schwaller, Gravitational Waves from a Dark Phase Transition, Phys. Rev. Lett. **115**, 181101 (2015).

[11] F. P. Huang and X. Zhang, Probing the gauge symmetry breaking of the early Universe in 3-3-1 models and beyond by gravitational waves, Phys. Lett. B **788**, 288 (2019).

[12] F. P. Huang and Jiang-Hao Yu, Exploring inert dark matter blind spots with gravitational wave signatures, Phys. Rev. D **98**, 095022 (2018).

[13] S. V. Demidov, D. S. Gorbunov, and D. V. Kirpichnikov, Gravitational waves from phase transition in split NMSSM, Phys. Lett. B **779**, 191 (2018).

[14] K. Hashino, M. Kakizaki, S. Kanemura, P. Ko, and T. Matsui, Gravitational waves from first order electroweak phase transition in models with the $U(1)_X$ gauge symmetry, J. High Energy Phys. 06 (2018) 088.

[15] N. Okada and O. Seto, Probing the seesaw scale with gravitational waves, Phys. Rev. D **98**, 063532 (2018).

[16] E. Madge and P. Schwaller, Leptophilic dark matter from gauged lepton number: Phenomenology and gravitational wave signatures, J. High Energy Phys. 02 (2019) 048.

[17] A. Ahriche, K. Hashino, S. Kanemura, and S. Nasri, Gravitational waves from phase transitions in models with charged singlets, Phys. Lett. B **789**, 119 (2019).

[18] V. Brdar, A. J. Helmboldt, and J. Kubo, Gravitational waves from first-order phase transitions: LIGO as a window to unexplored seesaw scales, J. Cosmol. Astropart. Phys. 02 (2019) 021.

[19] D. Croon, T. E. Gonzalo, and G. White, Gravitational waves from a Pati-Salam phase transition, J. High Energy Phys. 02 (2019) 083.

[20] A. Angelescu and P. Huang, Multistep strongly first order phase transitions from new fermions at the TeV scale, Phys. Rev. D **99**, 055023 (2019).

[21] T. Hasegawa, N. Okada, and O. Seto, Gravitational waves from the minimal gauged $U(1)_{B-L}$ model, Phys. Rev. D **99**, 095039 (2019).

[22] P. S. B. Dev, F. Ferrer, Y. Zhang, and Y. Zhang, Gravitational waves from first-order phase transition in a simple axionlike particle model, J. Cosmol. Astropart. Phys. 11 (2019) 006.

[23] V. Brdar, L. Graf, A. J. Helmboldt, and X.-J. Xu, Gravitational waves as a probe of left-right symmetry breaking, J. Cosmol. Astropart. Phys. 12 (2019) 027.

[24] X. Wang, F. P. Huang, and X. Zhang, Gravitational wave and collider signals in complex two-Higgs doublet model with dynamical CP-violation at finite temperature, Phys. Rev. D **101**, 015015 (2020).

[25] A. Greljo, T. Opferkuch, and B. A. Stefanek, Gravitational Imprints of Flavor Hierarchies, Phys. Rev. Lett. **124**, 171802 (2020).

[26] A. Von Harling, B. Pomarol, O. Pujolas, and F. Rompineve, Peccei-Quinn phase transition at LIGO, J. High Energy Phys. 04 (2020) 195.

[27] E. Hall, T. Konstandin, R. McGehee, H. Murayama, and G. Servant, Baryogenesis from a dark first-order phase transition, J. High Energy Phys. 04 (2020) 042.

[28] X. Wang, F. P. Huang, and X. Zhang, Phase transition dynamics and gravitational wave spectra of strong first-order phase transition in supercooled Universe, J. Cosmol. Astropart. Phys. 05 (2020) 045.

[29] W.-C. Huang, F. Sannino, and Z.-W. Wang, Gravitational waves from Pati-Salam dynamics, Phys. Rev. D **102**, 095025 (2020).

[30] N. Okada, O. Seto, and H. Uchida, Gravitational waves from breaking of an extra $U(1)$ in $SO(10)$ grand unification, arXiv:2006.01406.

[31] B. Fornal, Gravitational wave signatures of lepton universality violation, arXiv:2006.08802 [High Energy Phys (to be published)].

[32] J. J. Blanco-Pillado and K. D. Olum, Stochastic gravitational wave background from smoothed cosmic string loops, Phys. Rev. D **96**, 104046 (2017).

[33] C. Ringeval and T. Suyama, Stochastic gravitational waves from cosmic string loops in scaling, J. Cosmol. Astropart. Phys. 12 (2017) 027.

[34] Y. Cui, M. Lewicki, D. E. Morrissey, and J. D. Wells, Cosmic archaeology with gravitational waves from cosmic strings, Phys. Rev. D **97**, 123505 (2018).

[35] Y. Cui, M. Lewicki, D. E. Morrissey, and J. D. Wells, Probing the pre-BBN universe with gravitational waves from cosmic strings, J. High Energy Phys. 01 (2019) 081.

[36] G. S. F. Guedes, P. P. Avelino, and L. Sousa, Signature of inflation in the stochastic gravitational wave background generated by cosmic string networks, Phys. Rev. D **98**, 123505 (2018).

[37] J. A. Dror, T. Hiramatsu, K. Kohri, H. Murayama, and G. White, Testing the Seesaw Mechanism and Leptogenesis with Gravitational Waves, Phys. Rev. Lett. **124**, 041804 (2020).

[38] Y. Gouttenoire, G. Servant, and P. Simakachorn, Beyond the standard models with cosmic strings, J. Cosmol. Astropart. Phys. 07 (2020) 032.

[39] Y. Gouttenoire, G. Servant, and P. Simakachorn, BSM with cosmic strings: Heavy, up to EeV mass, unstable particles, J. Cosmol. Astropart. Phys. 07 (2020) 016.

[40] W. Buchmuller, V. Domcke, H. Murayama, and K. Schmitz, Probing the scale of grand unification with gravitational waves, Phys. Lett. B **809**, 135764 (2020).

[41] S. F. King, S. Pascoli, J. Turner, and Y.-L. Zhou, Gravitational waves and proton decay: Complementary windows into GUTs, arXiv:2005.13549.

[42] R. Zhou and L. Bian, Gravitational waves from cosmic strings and first-order phase transition, arXiv:2006.13872.

[43] M. Duerr and M. B. F. Perez, and P. Wise, Gauge Theory for Baryon and Lepton Numbers with Leptoquarks, Phys. Rev. Lett. **110**, 231801 (2013).

[44] T. Banks and N. Seiberg, Symmetries and strings in field theory and gravity, Phys. Rev. D **83**, 084019 (2011).

[45] A. Pais, Remark on baryon conservation, Phys. Rev. D **8**, 1844 (1973).

[46] S. Rajpoot, Gauge symmetries of electroweak interactions, Int. J. Theor. Phys. **27**, 689 (1988).

[47] R. Foot, G. C. Joshi, and H. Lew, Gauged baryon and lepton numbers, Phys. Rev. D **40**, 2487 (1989).

[48] C. D. Carone and H. Murayama, Realistic models with a light U(1) gauge boson coupled to baryon number, Phys. Rev. D **52**, 484 (1995).

[49] H. Georgi and S. L. Glashow, Decays of a leptophobic gauge boson, Phys. Lett. B **387**, 341 (1996).

[50] P. F. Perez and M. B. Wise, Baryon and lepton number as local gauge symmetries, Phys. Rev. D **82**, 011901 (2010); Erratum, Phys. Rev. D **82**, 079901 (2010).

[51] P. Schwaller, T. M. P. Tait, and R. Vega-Morales, Dark matter and vectorlike leptons from gauged lepton number, Phys. Rev. D **88**, 035001 (2013).

[52] P. F. Perez, S. Ohmer, and H. H. Patel, Minimal theory for lepto-baryons, Phys. Lett. B **735**, 283 (2014).

[53] M. Duerr and P. F. Perez, Theory for baryon number and dark matter at the LHC, Phys. Rev. D **91**, 095001 (2015).

[54] J. M. Arnold, P. F. Perez, B. Fornal, and S. Spinner, B and L at the supersymmetry scale, dark matter, and R-parity violation, Phys. Rev. D **88**, 115009 (2013).

[55] B. Fornal, A. Rajaraman, and T. M. P. Tait, Baryon number as the fourth color, Phys. Rev. D **92**, 055022 (2015).

[56] B. Fornal and T. M. P. Tait, Dark matter from unification of color and baryon number, Phys. Rev. D **93**, 075010 (2016).

[57] P. F. Perez and S. Ohmer, Unification and local baryon number, Phys. Lett. B **768**, 86 (2017).

[58] B. Fornal, Y. Shirman, T. M. P. Tait, and J. R. West, Asymmetric dark matter and baryogenesis from $SU(2)_\ell$, Phys. Rev. D **96**, 035001 (2017).

[59] N. Aghanim et al. (Planck Collaboration), Planck 2018 results. VI. Cosmological parameters, Astron. Astrophys. **641**, A6 (2020).

[60] P. F. Perez, E. Golias, R.-H. Li, C. Murgui, and A. D. Plascencia, Anomaly-free dark matter models, Phys. Rev. D **100**, 015017 (2019).

[61] T. W. B. Kibble, Topology of cosmic domains and strings, J. Phys. A **9**, 1387 (1976).

[62] A. Vilenkin and E. P. S. Shellard, *Cosmic Strings and Other Topological Defects* (Cambridge University Press, Cambridge, England, 2000).

[63] P. A. R. Ade et al. (Planck Collaboration), Planck 2013 results. XXV. Searches for cosmic strings and other topological defects, Astron. Astrophys. **571**, A25 (2014).

[64] T. W. B. Kibble, Evolution of a system of cosmic strings, Nucl. Phys. **B252,** 227 (1985); Erratum, Nucl. Phys. **B261,** 750 (1985).

[65] D. P. Bennett and F. R. Bouchet, Evidence for a Scaling Solution in Cosmic-String Evolution, Phys. Rev. Lett. **60,** 257 (1988).

[66] D. P. Bennett and F. R. Bouchet, Cosmic-String Evolution, Phys. Rev. Lett. **63,** 2776 (1989).

[67] A. Albrecht and N. Turok, Evolution of cosmic string networks, Phys. Rev. D **40,** 973 (1989).

[68] B. Allen and E. P. S. Shellard, Cosmic-String Evolution: A Numerical Simulation, Phys. Rev. Lett. **64,** 119 (1990).

[69] M. B. Hindmarsh and T. W. B. Kibble, Cosmic strings, Rep. Prog. Phys. **58,** 477 (1995).

[70] K. D. Olum and J. J. Blanco-Pillado, Radiation from Cosmic String Standing Waves, Phys. Rev. Lett. **84,** 4288 (2000).

[71] J. N. Moore, E. P. S. Shellard, and C. J. A. P. Martins, On the evolution of Abelian-Higgs string networks, Phys. Rev. D **65,** 023503 (2001).

[72] J. J. Blanco-Pillado, K. D. Olum, and B. Shlaer, The number of cosmic string loops, Phys. Rev. D **89,** 023512 (2014).

[73] T. Vachaspati and A. Vilenkin, Gravitational radiation from cosmic strings, Phys. Rev. D **31,** 3052 (1985).

[74] C. J. A. P. Martins and E. P. S. Shellard, String evolution with friction, Phys. Rev. D **53,** R575 (1996).

[75] C. J. A. P. Martins and E. P. S. Shellard, Quantitative string evolution, Phys. Rev. D **54,** 2535 (1996).

[76] C. J. A. P. Martins and E. P. S. Shellard, Extending the velocity dependent one scale string evolution model, Phys. Rev. D **65,** 043514 (2002).

[77] H.-K. Guo, K. Sinha, D. Vagie, and G. White, Phase transitions in an expanding Universe: Stochastic gravitational waves in standard and non-standard histories, arXiv:2007.08537.

[78] A. D. Linde, Decay of the false vacuum at finite temperature, Nucl. Phys. **B216,** 421 (1983).

[79] J. R. Espinosa, T. Konstandin, J. M. No, and G. Servant, Energy budget of cosmological first-order phase transitions, J. Cosmol. Astropart. Phys. 06 (2010) 028.

[80] M. Hindmarsh, S. J. Huber, K. Rummukainen, and D. J. Weir, Gravitational Waves from the Sound of a First Order Phase Transition, Phys. Rev. Lett. **112,** 041301 (2014).

[81] C. Caprini *et al.*, Science with the space-based interferometer eLISA. II: Gravitational waves from cosmological phase transitions, J. Cosmol. Astropart. Phys. 04 (2016) 001.

[82] M. Hindmarsh, S. J. Huber, K. Rummukainen, and D. J. Weir, Shape of the acoustic gravitational wave power spectrum from a first order phase transition, Phys. Rev. D **96,** 103520 (2017); Erratum, Phys. Rev. D **101,** 089902 (2020).

[83] J. Ellis, M. Lewicki, and J. M. No, On the maximal strength of a first-order electroweak phase transition and its gravitational wave signal, J. Cosmol. Astropart. Phys. 04 (2019) 003.

[84] C. Caprini *et al.*, Detecting gravitational waves from cosmological phase transitions with LISA: An update, J. Cosmol. Astropart. Phys. 03 (2020) 024.

[85] A. Kosowsky, M. S. Turner, and R. Watkins, Gravitational radiation from colliding vacuum bubbles, Phys. Rev. D **45,** 4514 (1992).

[86] S. J. Huber and T. Konstandin, Gravitational wave production by collisions: More bubbles, J. Cosmol. Astropart. Phys. 09 (2008) 022.

[87] M. Kamionkowski, A. Kosowsky, and M. S. Turner, Gravitational radiation from first order phase transitions, Phys. Rev. D **49,** 2837 (1994).

[88] K. Yagi and N. Seto, Detector configuration of DECIGO/ BBO and identification of cosmological neutron-star binaries, Phys. Rev. D **83,** 044011 (2011); Erratum, Phys. Rev. D **95,** 109901 (2017).

[89] B. Sathyaprakash *et al.*, Scientific objectives of Einstein Telescope, Classical Quantum Gravity **29,** 124013 (2012) , Erratum, Classical Quantum Gravity **30,** 079501 (2013).